Vehicle Anti-Skid Control by Means of Extended State Observer and Active Disturbance Rejection Controller

[1]Paul P. Lin, [2]Masheng Ye and [3]Kuo-Ming Lee

Abstract

When the driving road surface condition suddenly changes from dry to wet, the driving wheels will slip due to much lower coefficient of friction, and thus cause the vehicle to skid. Unlike the popular anti-brake system which applies differential braking to wheels, the presented ant-skid Control properly distributes torques to wheels without braking. In comparison with many recently developed anti-skid control systems, the presented ant-skid control scheme does not require the knowledge of the does not require knowledge of the exact vehicle model, and can reject disturbance and unknown dynamics. More specifically, the anti-skid control is achieved by employing Extended State Observer (ESO) and Active Disturbance Rejection Control (ADRC) algorithm that treats any discrepancy between the exact and the unknown nonlinear or time-varying plant as disturbance to be estimated and rejected The objective of the anti-skid control is to control the vehicle's yaw motion at the center of mass by closely following the desired yaw rate regardless of cornering or road surface condition. The simulation results show that the anti-skid control is very effective in maintaining the vehicle stability during cornering on a split-μ road surface (i.e. the left side on dry surface, while the right side on icy surface).

Keywords-Extended state observer; Anti-skid control; Active disturbance rejection control

[1]*ASME Fellow, Professor & Asso. Dean,*
Dept. of Mechanical Engineering, Cleveland State University, USA
[2]*Mechanical System Engineer, Caitin, Inc.*
San Francisco, California, USA
[3]*General Manager, X-Ball Technology, Nanzu, Kaohsiung, Taiwan*
Email:paulplin@hotmail.com

1. Introduction

Passive systems for vehicle safety control has been investigated by many researchers and developed by the automobile manufacturers. In the passive vehicle control family, several technologies have found their way into production commercial vehicles, such as Anti-Brake Systems (ABS), Traction Control (TC), and Vehicle Stability Control (VSC). The ABS system is designed to prevent vehicle wheel skidding during braking, whereas the TC system is to prevent vehicle wheel skidding during acceleration. VSC is a technology of applying electronic control to vehicles. It was developed to improve the vehicle safety by preventing vehicles from spinning and drifting out with proper control system design. It is also referred to as yaw stability control system or electronic stability control systems. Anti-skid control (ASC) presented in this paper can be classified under the category of VSC technology. In other words, the ASC is more specific about skid preventing due to a sudden road surface change, while the VSC is more about maintaining the vehicle stability

When a vehicle is cornering without proper control, the vehicle's trajectory could be greatly affected by the road surface condition. As the road surface's friction coefficient suddenly becomes very small, the driving wheels will slip, which will likely cause the vehicle to skid. There have been several ways to minimize skidding by means of controlling the vehicle's yaw motion. They are such as differential braking systems, and steer-by-wire systems, etc. The differential braking systems utilize the ABS brake

system on the vehicle to apply differential braking between the left and right wheels to control yaw rate, while the steer-by-wire systems track the driver's steering angle input by adding an assistant steering angle to the wheels. However, applying differential braking on a road is undesired as it may cause accidents. The steer-by-wire system has not been proven effective since controlling steering angle alone is not sufficient in preventing the vehicle from skidding.

In terms of vehicle stability control, some methods based on slip ratio estimation have been developed. Fujimoto, et. al. in [1] proposed a method for estimating the slip ratio to control the vehicle by properly distributing the torque based on wheel's slip ratio. Hallowell and Ray [2] developed a traction control algorithm by using independent torque control on each wheel. The traction control system reduces the engine torque or applies brakes to the slipping wheels and brings the slipping wheels into the desirable skid range. Later, Osborn and Shim [3] developed independent control of all-wheel-drive torque distribution using proportional-integral control strategy by applying yaw rate feedback to vary the front-rear torque distribution and lateral acceleration feedback to adjust the left-right distribution. In terms of vehicle anti-skid control, Kececi and Tao [4] developed an adaptive control technique that keeps the speed of the vehicle as desired by applying more power to the drive wheels where the additional driving force at the non-skidding wheel will compensate for the driving force at the skidding wheel, and also arranges the direction of the vehicle motion by changing the steering angle of the two front steering wheels. As mentioned in [4], in many existing skid control systems, the skidding wheel is detected and power applied to this wheel is reduced until traction is

regained. However, after the skidding occurs, in order to regain control of the vehicle, the vehicle speed is reduced, which presents a safety problem when traveling on a heavy traffic road. The common drawback of these control methods, however, is the necessity of knowing the vehicle model. Even in the assumed vehicle model, air resistance, load transfer between the axles, suspension system dynamics, vaster effect and tire dynamics are often not included. This paper proposes a new anti-skid control scheme by means of Active Disturbance Rejection Controller (ADRC) that does not require knowledge of the exact vehicle model, and can reject disturbance and unknown dynamics. The presented technique minimizes skid by properly distributing torque to each wheel without braking.

This paper is arranged in five sections. Section I introduces vehicle stability control techniques along with the significance of vehicle anti-skid control. Section II introduces the vehicle dynamic system modeling, while Section III introduces velocity and yaw rate estimation via Extended State Observer (ESO). Section IV describes the ADRC-based anti-skid controller design. Section V shows computer simulation results. Finally, the conclusions are given in Section VI.

2. Vehicle dynamics modeling

The vehicle under study is four-wheel drive with independent torque distribution, as shown in Fig. 1.

Without considering air resistance, load transfer between the axles, and some other disturbances, the dynamic equations for the vehicle's longitudinal acceleration, lateral acceleration and yaw angular acceleration, respectively can be derived using the Newton's law.

$$m\dot{V}_x = m\gamma V_y + F_{LLF}\cos\delta + F_{LRF}\cos\delta - F_{SLF}\sin\delta - F_{SRF}\sin\delta$$
$$+F_{LLR} + F_{LRR}$$

$$m\dot{V}_y = -m\gamma V_x + F_{LLF}\sin\delta + F_{LRF}\sin\delta + F_{SLF}\cos\delta + F_{SRF}\cos\delta$$
$$+F_{SLR} + F_{SRR}$$

$$J\dot{\gamma} = (F_{LRF}\cos\delta - F_{LLF}\cos\delta + F_{LRR} - F_{LLR} + F_{SLF}\sin\delta - F_{SRF}\sin\delta)l_t$$
$$+(F_{LLF}\sin\delta + F_{LRF}\sin\delta + F_{SLF}\cos\delta + F_{SRF}\cos\delta)l_f - (F_{SLR} + F_{SRR})l_r$$

$$(1)$$

Where m is the vehicle's total mass, J is mass moment of inertia at the vehicle's center of mass. When the vehicle is cornering, the longitudinal velocity of each wheel is no longer the same. The longitudinal velocity of the right and left front wheels ($V_{x,WRF}$ and Vx,WLF, respectively) and that of the right and left rear wheel ($V_{x,WRR}$ and $V_{x,WLR}$, respectively) can be calculated by

$$V_{x,WRF} = (V_x + \gamma l_t)\cos\delta + (V_y + \gamma l_f)\sin\delta$$
$$V_{x,WLF} = (V_x - \gamma l_t)\cos\delta + (V_y + \gamma l_f)\sin\delta$$
$$V_{x,WRR} = V_x + \gamma l_t$$
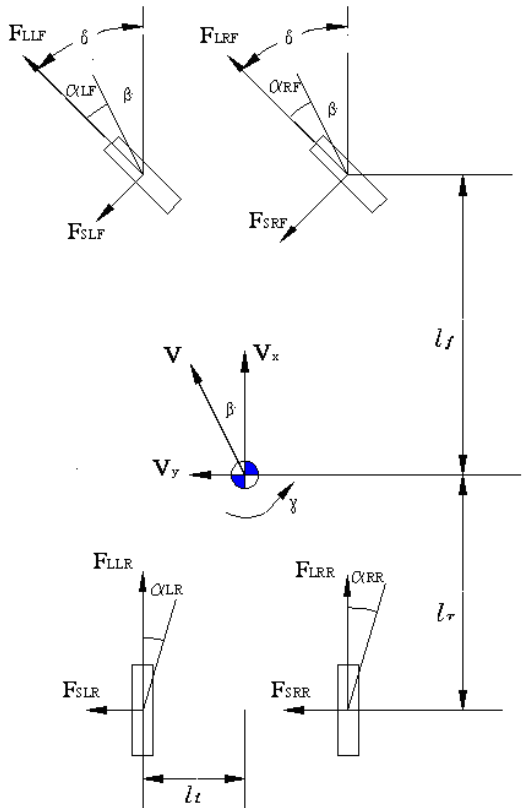$$V_{x,WLR} = V_x - \gamma l_t$$

$$(2)$$

Figure 1: Vehicle Schematics

These wheel longitudinal velocities can then be used to calculate the slip ratio of each wheel if the rotating speed of each wheel is known. This speed can be estimated as to be described in the next section, or obtained from the wheel speed sensors equipped in anti-brake systems (ABS). The slip ratio at axle i and side wheel j, σij, can be calculated by

$$\sigma_{ij} = \left| \frac{\omega_{ij}R - V_{x,Wij}}{\max(\omega_{ij}R, V_{x,Wij})} \right| \qquad (3)$$

Where ω_{ij} is the rotating speed of wheel j at axle i, and R is the tire radius.

3. Velocity and yaw estimation via extended state observer

The ability to effectively estimate the vehicle's velocity and yaw rate in real time is crucial to anti-skid control. The velocity of a vehicle can be measured by a GPS device which often contains signal noise and drift [5]. The yaw rate can also be measured by a MEMS yaw rate sensor. Alternatively, the velocities and yaw rate can be estimated by means of an observer. However, the existing observers are either designed for linear systems or requiring substantial knowledge of the dynamic system model. To overcome the drawbacks, this study proposes using a nonlinear observer called Extended State Observer (ESO).

3.1 Introduction to Extended State Observer

Since the dynamic model of a vehicle is highly nonlinear and time varying, an observer is needed to estimate the system's states. Extended State Observer (ESO) is introduced, which can augment both unknown dynamics and disturbances as an extended state and estimate it in real time by using input-output data. The ESO concept was first proposed by Han in

[6]. However, it was rather complex due to necessity of adjustments or tuning of several parameters, which can be difficult and time consuming. Later, Gao [7] improved the ESO technique and made it more practical by using a particular parameterization method that reduces the number of tuning parameters to one.

For a general first-order plant, the dynamic equation can be written as

$$\dot{y} = f + bu \qquad (4)$$

where y is the system output, f can be viewed as the generalized disturbance, u is the system or control input and b is a constant. The state space of the system can be represented in the following form:

$$\begin{cases} \dot{x}_1 = x_2 + bu \\ \dot{x}_2 = h = \dot{f} \\ y = x_1 \end{cases} \qquad (5)$$

Where x_1 is the original state and x_2 is the augmented state denoted as f. In this study, the term "f" is referred to as the system general dynamics. Alternatively, (9) can be expressed in matrix form as

$$\begin{cases} \dot{x} = Ax + Bu + Eh \\ y = Cx \end{cases} \qquad (6)$$

Where

$$x = \begin{bmatrix} x_1 \\ x_2 \end{bmatrix}; A = \begin{bmatrix} 0 & 1 \\ 0 & 0 \end{bmatrix}; B = \begin{bmatrix} b \\ 0 \end{bmatrix}; C = \begin{bmatrix} 1 & 0 \end{bmatrix};$$

$$E = \begin{bmatrix} 0 \\ 1 \end{bmatrix}$$

The state space observer can be constructed as

$$\begin{cases} \dot{z} = Az + Bu + L(y - \hat{y}) \\ \hat{y} = Cz \end{cases} \qquad (7)$$

$$(7)$$

Here is the estimation of the system output y, and L is a set of nonlinear gain [6], which was greatly simplified by Gao [7] with a single tuning parameter (i.e. observer bandwidth), which can be obtained using any known method such as the pole placement technique.

$$L = [\beta_1 \ \beta_2]^T = [2\omega_o \quad \omega_o^2]^T \qquad (8)$$

Here the ω_o is known as the *observer bandwidth*.

3.2 Estimation of Vehicle Velocity and Yaw Rate at Center of Mass

The torques applied to each wheel plays a key role in controlling the vehicle's stability, and they are, indeed, the control inputs. However, the vehicle's dynamic equations as shown in (1) are involved only with forces. Thus, it is essential for each wheel to relate the applied torque to the driving force. The relationship between them can be described by

$$\tau_{ij} - RF_{Lij} = J_\omega \dot{\omega} \qquad (9)$$

Where τ_{ij} is the applied torque on axle i and side wheel j, R is the wheel radius, F_{Lij} is the longitudinal force to be defined later, J_ω is the wheel's mass moment of inertia, and $\dot{\omega}$ is the wheel's angular acceleration. The applied torque affects the wheel's angular acceleration, which in turn, affects the wheel's slip ratio. The slip ratio ultimately affects the wheel's longitudinal and lateral forces used in (1).

4. ADRC-based anti-skid controller design

The proposed anti-skid control is achieved by using Active Disturbance Rejection Controller, known as ADRC. It was originally proposed by Han in [8] for nonlinear control. Few years later, Gao [9] simplified the control law and tuning method. Sun and Gao [10] successfully applied a DSP-based ADRC for a 1-kw H-bridge DC-DC power converter. Later, Sun [11] presented comments on ADRC in four aspects: (1) tracking differentiator, (2) nonlinear combination of proportional, integral, and differential errors, (3) extended state observer, and (4) disturbance rejection, and concluded that ADRC might not necessarily require tracking differentiator

and/or nonlinear gains by actively estimating and rejecting disturbance and unknown dynamics. More recently, Dong and Avanesian [12] presented drive-mode control for vibrational MEMS Gyroscopes using ADRC. In their study, the stability and robustness of the control systems were successfully justified through frequency-domain analysis.

4.1 How ADRC works

ADRC is a new design methodology that uses a very simple model, typically an integrator or a double integrator for a first-order or second-order system, for the controller design and treat any discrepancy between this model and the unknown, nonlinear or time-varying plant as disturbance to be estimated and rejected. The result is a high performance control system that is tuned only with one parameter: the bandwidth. The ADRC is built by using the feedback states which can be observed by the ESO described earlier.   For a general second-order plant, the dynamics equation can be written as

$$\ddot{y} = f + b_0 u \qquad (10)$$

The basic idea is to find an estimate of f, denoted as $\hat{f}$, and use it in the control law as

$$u = (u_0 - \hat{f})/b_0 \qquad (11)$$

Substituting (21) into (20), the control law reduces the original plant to an integral plant

$$\ddot{y} = (f - \hat{f}) + u_0 \approx u_0 \qquad (12)$$

which can be easily controlled by a Proportional-Derivative (PD) controller as

$$u_0 = k_p(r - \hat{y}) - k_d \dot{\hat{y}} \qquad (13)$$

Where r and $\hat{y}$ is the reference and estimated outputs, respectively, $\dot{\hat{y}}$ is the time derivative of $\hat{y}$, and k_p and k_d are the proportional and derivative controller gains, respectively. These controller gains can be selected as $k_p = \omega_c{}^2$ and $k_d = 2\zeta\omega_c$ where ω_c and ζ are the desired close-loop natural frequency and damping ratio, respectively. The ω_c is usually chosen as 1/5 to 1/3 of the observer bandwidth ω_o. The controlled input can then be expressed by

$$u = \frac{k_p(r - \hat{y}) - k_d \dot{\hat{y}} - \hat{f}}{b_0} \qquad (14)$$

Likewise, a general first-order plant can be controlled by a Proportional (P) controller. In summary, the ADRC constantly estimates the system general dynamics, treats the discrepancy between the actual and estimated plant as disturbance, and actively rejects that disturbance in real time. The control effectiveness relies on how accurate the ESO estimates the general dynamics.   It is worthwhile to note that one of the authors has mathematically proved that the ESO's estimation error is upper-bounded as long as the selected bandwidth, ω_o is sufficiently large. Coincidentally, the study on drive-mode control for vibrational MEMS gyroscopes [12] also found that the tracking error between the actual output and the reference signal for the drive mode converged with the increase of the controller's bandwidth.

4.2 Control objective

When a vehicle is driven straight on dry road surface, the vehicle's yaw rate is near zero. But when the vehicle is driven on low-friction road surface or during cornering, the vehicle needs to follow a guideline known as the desired yaw rate for steady state.   The anti-skid controller uses the desired yaw rate value as reference, and rejects all system dynamics and external disturbances other than the

vehicle yaw rate. Thus, the control objective is to track the actual yaw rate and minimize its deviation from the desired yaw rate. In this study, the bank angles on a slant road and vehicle yaw resonation are neglected. The desired yaw rate for steady state can be calculated by the following formula [13].

$$\gamma_{desired} = \frac{V_x \delta}{(l_f + l_r)(1 + \frac{V_x^2}{V_x^2 + V_y^2})} \qquad (15)$$

Where δ is the steering angle (the driver's input), l_f is the distance between the vehicle's center of mass (C.M.) and the front wheel axle, l_r is the distance between the vehicle's C.M. and the rear wheel axle, and V_x and V_y are the vehicle's longitudinal and lateral velocities, respectively.

4.3 Required total torque and torque distribution

The required torque for a vehicle has been defined by Osborn and Shim [14] as

$$T_{total} = mR\sqrt{(\mu g)^2 - a_y^2} \qquad (16)$$

The calculated total torque is constantly checked to make sure that it does not exceed the maximum torque available for a vehicle. Since yaw rate is the only control objective, this anti-skid controller works only when the vehicle skids, which in other words, having a non-zero yaw rate.

It can be reasoned that a smaller torque should be applied to the wheel that has a larger slip ratio. Furthermore, no torque should be applied to any wheel which completely slips (i.e. with slip ratio of 1). This leads to a torque distribution algorithm which states that the extent of torque distribution should be inversely proportional to the wheel slip ratio. Thus, four individual controller gains K_{RF}, K_{RR}, K_{LF} and K_{LR}, one for each wheel, were added in the controller. These gains can be calculated by

$$K_{ij} = K\frac{1 - \sigma_{ij}}{\sum \sigma} \qquad (17)$$

Where K_{ij} is the torque distribution gain for the axle i and side j wheel; K is the proportional gain; σ_{ij} is the slip ratio of axle i side j wheel; $\sum \sigma$ is the sum of four slip ratios of the wheels.

5. Simulation results

The proposed anti-skid control was simulated using Matlab/Simulink for 10 seconds. During this time period, the vehicle turned and encountered one-wheel skid while turning.

During $0 \leqslant t \leqslant 2$ sec., the vehicle is driven straight on dry-road surface.

During $2 < t \leqslant 10$ sec. the vehicle starts to turn counter-clockwise for 1 radian (~57.3°).

At t = 6 sec, the vehicle enters a split-μ road (i.e. the left-side wheels on dry surface with coefficient of friction μ =1.0 while the right-side whiles on icy surface with coefficient of friction μ=0.2).

The simulation gives comparisons of yaw rate and vehicle course to demonstrate how the vehicle's skid is controlled by the presented technique.

5.1 Yaw rate comparison

The control objective is to make the vehicle closely follow the desired yaw rate. Fig. 2 shows the comparison between the desired yaw rate for steady state and the actual yaw rate without control. As it can be seen, without control the vehicle begins to deviate from the desired yaw rate (30° per second) as soon as it turns at t=2 sec.
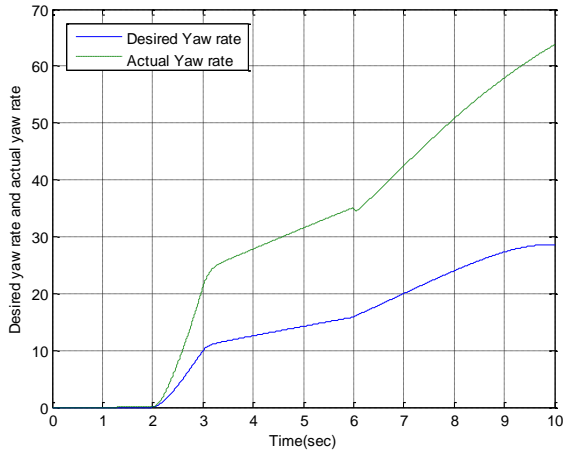
Figure 2: Desired yaw rate and actual yaw rate without control

5.2 Vehicle Course Comparison

The objective of anti-skid control is essentially to control the vehicle's yaw motion at the center of mass by closely following the desired yaw rate regardless of cornering or road surface condition. Thus, one way to verify the control effectiveness is to compare the vehicle course (or trajectory) with the referenced or desired one.

The actual vehicle course is defined as the sum of the vehicle's slip angle and the vehicle's yaw angle [9].

$$\psi = \beta + \varphi \qquad (18)$$

Where slip angle β is represented by

$$\beta = \arctan\left(\frac{V_y}{V_x}\right) \qquad (19)$$

Where φ is the vehicle's yaw angle which is the time integral of yaw rate γ. The vehicle course estimated by the ESO can be expressed as

$$\hat{\psi} = \hat{\beta} + \hat{\varphi} \qquad (20)$$

Where

$$\hat{\beta} = \arctan\left(\frac{\hat{V}_y}{\hat{V}_x}\right) \qquad (21)$$

Once again, the simulation assumes that vehicle was driven straight for the first two seconds, and then turned counter-clockwise for 1 radian (~57.3°). At t = 6 sec. while cornering, the vehicle encountered a split-μ road (i.e. the left side on dry surface while the right side on icy surface). Fig. 3 shows the comparison of vehicle course among three scenarios. Note that the vehicle course in this case is the reference steering angle which is 57.3°.
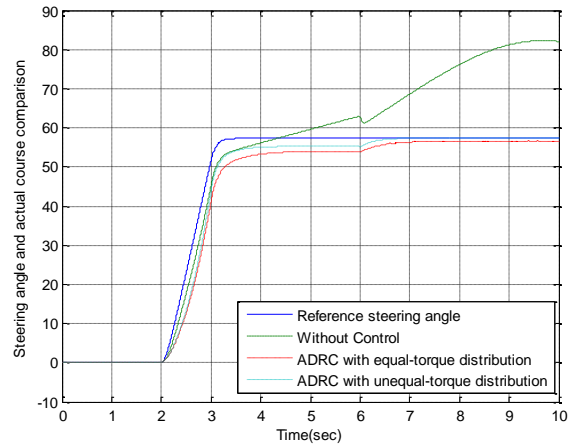

Figure 3: Control performance: vehicle course comparisons

The control performance in terms of vehicle course is further compared between the ADRC and PID controller, as shown in Fig. 4.
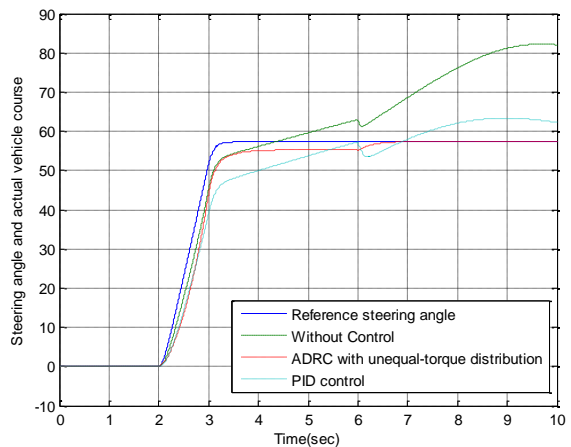

Figure 4: Control performance between ADRC and PID

Because of the poor robustness, the PID controller does not respond as quickly as ADRC does when road surface suddenly changes at t = 6 seconds. The PID controller also did not respond to the new steering angle at t = 2 seconds. At t =3 second, the PID controller responds slowly while the vehicle remains turning, and after the sudden change of surface at t = 6 second, the PID controller essentially overshoots the reference vehicle course. In contrast, the ADRC with unequal-torque distribution keeps the vehicle under control all the time by rejecting external disturbances.

6. Conclusions

The presented Extended State Observer (ESO) plays an important role in this study in the sense that it augments both unknown dynamics and disturbances as an extended state and estimates it in real time by using input-output data. The Active Disturbance Rejection Control (ADRC) algorithm rejects the disturbance that includes the discrepancy between the exact and the unknown nonlinear or time-varying plant. By gracefully combining the ESO and ADRC, the presented anti-skid control demonstrated its ability to prevent the vehicle from skidding when encountering a split-μ road surface condition during cornering.

The ADRC-based anti-skid control essentially controls the vehicle's yaw motion by properly applying torque to each wheel without breaking. The control is achieved by minimizing the discrepancy between the estimated yaw rate and the desired yaw rate for steady state to prevent the vehicle from spinning about its center of mass. The anti-skid control scheme is particularly useful when the vehicle suddenly encounters a low friction coefficient road surface. In this case, the sudden change in vehicle

dynamics is treated as disturbance which is estimated in real time and subsequently rejected by the ADRC control law.

References

[1] H. Fujimoto, K. Fujii, and N. Takahashi, "Vehicle stability control of electric vehicle with slip-ratio and cornering stiffness estimation", Proc. of the IEEE/ASME Int. Conf. on Advanced Intelligent Mechatronics, 2007, pp.1-6.

[2] J. Hallowell and R. Ray, "All-wheel driving using independent torque control of each wheel," Proc. American Control Conf., Denver, CO, 2003, pp. 2590-2595.

[3] P. Osborn and T. Shim, "Independent control of all-wheel drive torque distribution," Vehicle System Dynamics, V44, N7, July 2006, pp.529-546.

[4] E. F. Kececi and G. Tao, "Adaptive vehicle skid Control," Mechatronics, 16, pp.291-301, 2006.

[5] D. M. Bevly, "Global positioning systems (GPS): a low-cost velocity sensor for correcting inertial sensor errors on ground vehicles," Trans. of the ASME, J. of Dynamic Systems, Measurement and Control, V126, pp. 255-264, 2004.

[6] J. Han, "A class of extended state observers for uncertain systems," Control and Decision, vol. 10, no. 1, pp. 85-88. (In Chinese), 1995.

[7] Z. Gao,"Scaling and parameterization based controller tuning," Proc. of the 2003 American Control Conference, V 6, June 2003, pp. 4989 – 4996.

[8] J. Han, "Nonlinear state error feedback control," Control and Decision, vol. 10, no. 3, pp. 221-225. (In Chinese), 1995.

[9] Z. Gao, "Active Disturbance Rejection Control: a Paradigm Shift in Feedback Control System Design," in: Proc. 2006 American Control Conference, Minneapolis, Minnesota, USA, 2006, pp. 4989-4996.

[10] B. Sun and Z. Gao, "A DSP-based active disturbance rejection control design for 1-kW H-bridge DC-DC power converter," IEEE Trans. Ind. Electron., vol. 52, no. 5, pp. 1271-1277, Oct. 2005.

[11] D. Sun, "Comments on active disturbance rejection control," IEEE Trans. Ind. Electron., vol. 54, no. 6, pp. 3428-3429, Dec. 2007.

[12] L. Dong and D. Avanesian, "Drive-mode control for vibrational MEMS Gyroscopes," IEEE Trans. Ind. Electron., vol.56, no. 4, pp. 956-963, April 2009.

[13] R. Rajamani, "Vehicle dynamics and control", Springer, ISBN: 0-387-26396-9, 2006, pp.429-441.

[14] P. Osborn and T. Shim, "Independent control of all-wheel drive torque distribution," Vehicle System Dynamics, vol. 44, no. 7, July 2006, pp. 529-546.